Parasitic oscillation in the low-frequency noise characterization of solar cells

Chloé Wulles, Quentin Rafhay, Thibaut Desrues, Anne Kaminski, Christoforos Theodorou

Parasitic oscillation in the low-frequency noise characterization of solar cells

Chloé Wulles[1], Quentin Rafhay[1], Thibaut Desrues[2], Anne Kaminski[1], Christoforos Theodorou[1]

[1]Univ. Grenoble Alpes, Univ. Savoie Mont Blanc, CNRS, Grenoble INP, IMEP-LAHC, 38000 Grenoble, France. Email : chloe.wulles@grenoble-inp.fr
[2]Univ. Grenoble Alpes, CEA, LITEN, DTS, SCPV, F-73370 Le Bourget-du-Lac

1. Abstract

The analysis of low-frequency noise in solar cells is a very useful tool for defect characterization or understanding of fluctuation mechanisms in photodiodes. This type of noise characterization can however be limited by the presence of an undesired peak in the frequency spectra, caused by an oscillation in the measured current. It is shown in this work that this phenomenon originates in the interaction between the noise measurement system and the test structures of the solar cells, which usually introduce a high parasitic capacitance. Through experimental measurements, the link between the center frequency of the peak and the sensitivity of the noise measurement amplifier, as well as the solar cell surface area were explored. Finally, it is shown that, for characterization purposes, the oscillation peak could be pushed to higher frequencies by measuring smaller area cells or attenuated by choosing electrode shapes that enhance the device series resistance.

2. Introduction

It is known that the performance of photovoltaic components is strongly influenced by the absorbing material quality and defects introduced during their manufacturing process, which may cause trap/carrier generation-recombination events. It is therefore important to enhance and further develop the tools used to detect and characterize these defects. For example, the measurement of electronic low frequency noise (LFN) is a non-destructive trap characterization tool that has been traditionally used for devices such as transistors [1], but that can be also exploited in photovoltaic devices [2], [3]. .

A valuable mathematical tool for the analysis of a component's LFN is the power spectral density (PSD), which shows the frequency distribution of the power of a signal. It is therefore crucial for the measurement to have no distortion or undesirable interferences for a large frequency bandwidth. However, conventional test structures for photovoltaic cells may be unsuitable for noise measurements, especially if the electronic circuit of the test set up has been optimized for measuring electronic components with a relatively low capacitance. Indeed, mainly due to their large surface area, solar cell test structures can introduce a high equivalent capacitance and affect the dynamic stability of the measurement.[4]. This can result in the appearance of a parasitic peak in the power spectral density spectra, which has been observed in some works [2],[3] without the authors commenting on them however. Apart from the fact that the spectrum values close to this peak frequency become unusable, the time domain signal is contaminated by this parasitic oscillation and cannot be used to extract information, such as in the case of Random Telegraph Noise [5], [6].

This paper presents a study of the influence of various parameters, such as the amplifier sensitivity, as well as the photodiode area and series resistance, on this parasitic oscillation effect. Finally, some suggestions are provided on which test structures have to be favored for the measurement of electronic noise in solar cells.

3. Experimental exploration

All test samples used in this work are Al-BSF solar cells fabricated at CEA-INES, for which more details can be found in [7]. Fig. 1-(a) shows the current PSD spectra obtained from two measurements in dark on a solar cell forward-biased at 5 mV and 25 mV. On both spectra, a peak spread around a frequency, f_o, of roughly 1600 Hz and with constant amplitude is observed. Its presence greatly reduces the frequency range over which the noise can be studied, especially when the LFN level is lower than the peak amplitude.

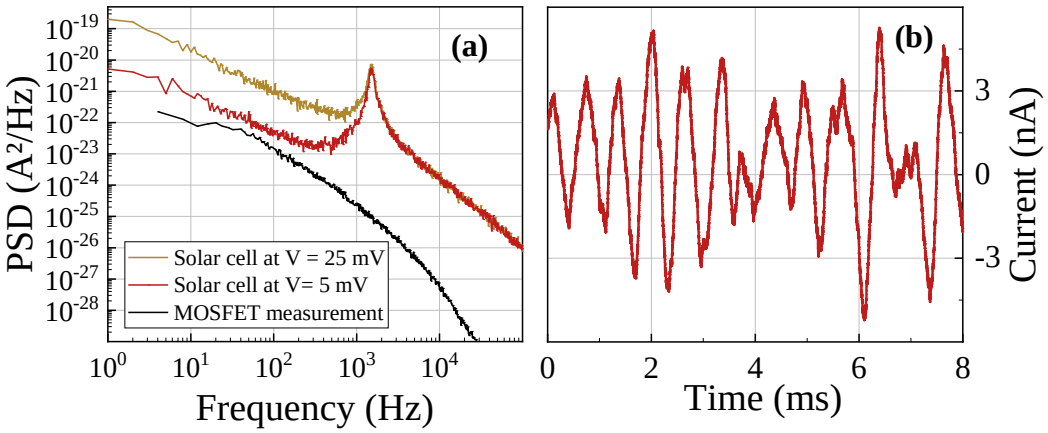

Figure 1: (a) Power spectral density versus frequency measured on a 6,25 cm² solar cell biased at 5 mV and 25 mV and **(b)** time series of AC current corresponding to the spectrum obtained at V = 5 mV .

An extract of the time domain acquisition of the current at V = 5 mV, presented in figure 1-(b), reveals an oscillation with irregular period and amplitude. The average period of this oscillation was extracted at about 620 µs, which corresponds well to f_o = 1600 Hz, spread out because of jitter/phase noise [8]. This finding, combined with the fact that this peak does not appear in measurements with MOSFET (see Fig. 1a) or simple p-n diode samples, led us to assume that it could be generated by the solar cell's parasitic L-C elements. However, as Fig. 2 shows, increasing the applied voltage led to f_o moving to higher frequencies, but staying constant for certain bias ranges.

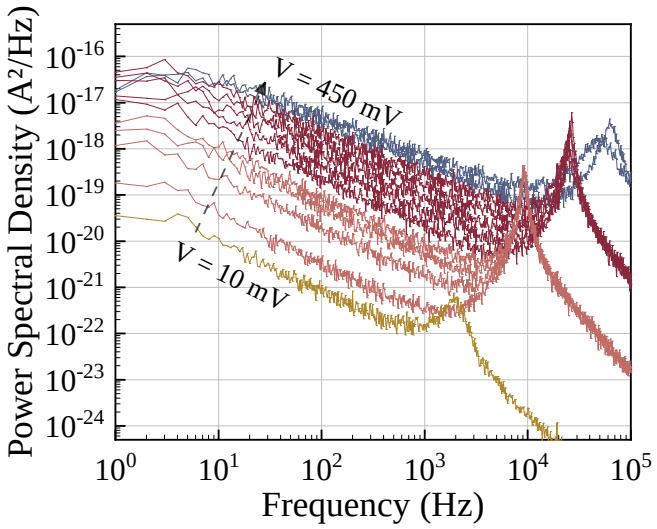

Figure 2: Power spectral densities measured on a 6,25 cm² cell with the applied voltage increasing from 10 mV to 450 mV.

The peak frequency was extracted for all gate bias values and is shown in Fig. 3, together with the corresponding amplifier sensitivity values. It becomes evident that the amplifier sensitivity is the one affecting f_o, and the latter does not seem to vary with bias for a given sensitivity. Therefore, the solar cell does not induce the oscillatory behavior itself, but rather in combination with the measurement system.

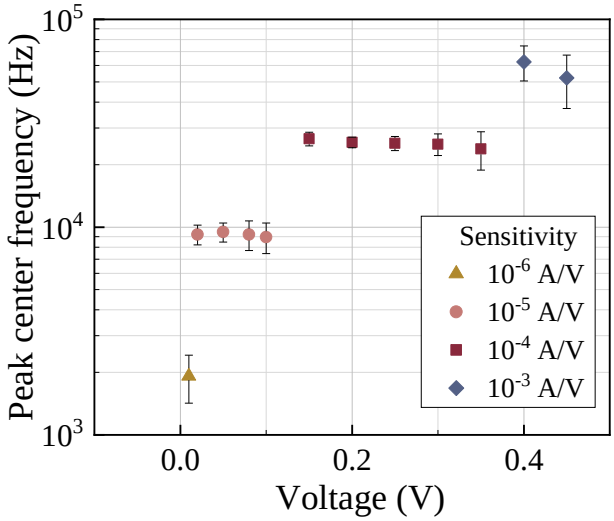

Figure 3 : Peak frequencies extracted from spectra presented in Fig. 2 as a function of the applied voltage.

The noise measurement is achieved through a programmable electronic box designed by the company "Synergie concepts" [9] and optimized for low frequency noise measurement applications on devices with low equivalent capacity. To better demonstrate how the measurement circuit can affect f_o, a simplified schematic diagram showing the general operation of the transimpedance (current-to-voltage) amplifier (TIA) used in our noise acquisition system is shown in Fig. 4. The C_d, R_d and R_s represent the photodiode's capacitance, shunt and series resistance respectively, whereas R_f defines the DC gain of the TIA and C_f is the feedback capacitance.

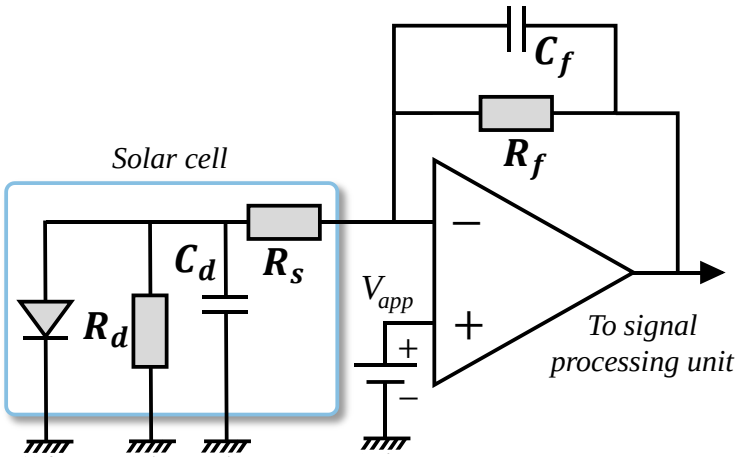

Figure 4: Equivalent circuit at the input of the measurement bench.

Each sensitivity range utilizes a different value of R_f and a carefully chosen value of C_f for compensation purposes, since the operational amplifier (OpAmp) used is not necessarily the same. As analytically demonstrated in [10], in photodiode amplifiers using the TIA approach to make use of the photo-generated current, the combination of the OpAmp's low-pass behavior and the photodiode's C_d can lead to an

oscillating behavior, with $f_o \propto 1/\sqrt{R_f C_d}$, because C_d introduces an inductance-like behavior by the way it is connected to the feedback loop. The generally accepted method to avoid this parasitic oscillation is to introduce C_f for compensation. However, in our case, where a pre-fabricated noise measurement system is utilized, the TIA has been already optimized regardless the device impedance, therefore C_f is fixed to a value thanks to which the oscillation is avoided when the device capacitance is relatively low. The authors did not have the possibility to modify elements of the circuit, since it is located in the interior of a measurement instrument fabricated by […]. By consequence, once C_d is connected during the measurement, it modifies the compensation achieved by C_f, making the oscillation re-appear at a frequency that is proportional to $1/\sqrt{R_f(C_d + C_f)}$ [10]. It is worth noting that apart from their use as current noise measurement tools, the TIA-based amplifier systems are also the typical solution for photodiode signal reading and manipulation as explained in [10], as they can convert the photo-generated current to a voltage signal, while at the same time providing isolation as a buffer circuit between the solar cell and the output signal. Therefore, the impedance matching issues between solar cells (photodiodes in general) and TIAs affecting the noise behavior concern also other types of applications [4,11–13].

4. Proposed solutions

A first obvious solution to eliminate the parasitic oscillation would be to adapt the values of the feedback capacitance C_f to compensate the oscillation induced by the solar cell. However, as mentioned earlier, these values are fixed in our measuring instrument. When designing a test bench dedicated to noise measurement on components with high equivalent capacitance, it is therefore recommended to choose relevant values of compensation capacitances, but in our case, the only immediate solution was to adapt the test structure to the noise measurement system.

Based on the above estimation, f_o was measured for various solar cell surface areas, *S*, obtained by different cutting methods. The spectra obtained are presented in Fig. 5, where the shift of the peak frequency with the diminution of the solar cell area is clearly visible. Values of f_o were then extracted so as $1/f_o^2$ could be plotted against device area.

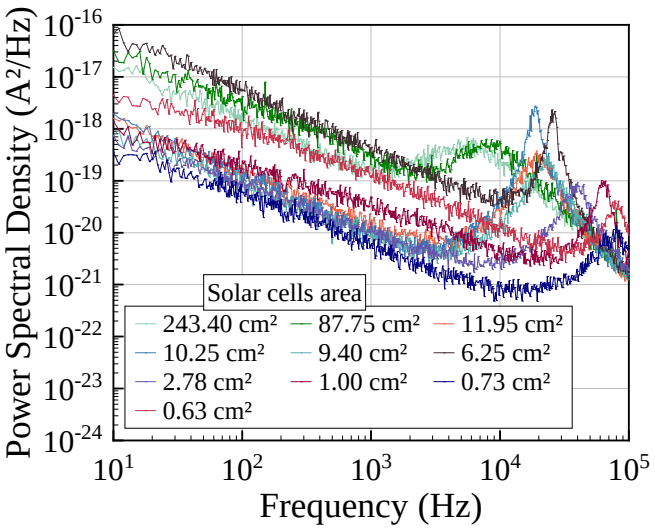

Figure 5: Power spectral density measured at the same sensitivity for various sizes of samples.

The results, shown in Fig. 6, are in agreement with $f_o \propto 1/\sqrt{R_f C_d}$, predicting a proportionality between these parameters since the solar cell capacitance is assumed to be proportional to its area.

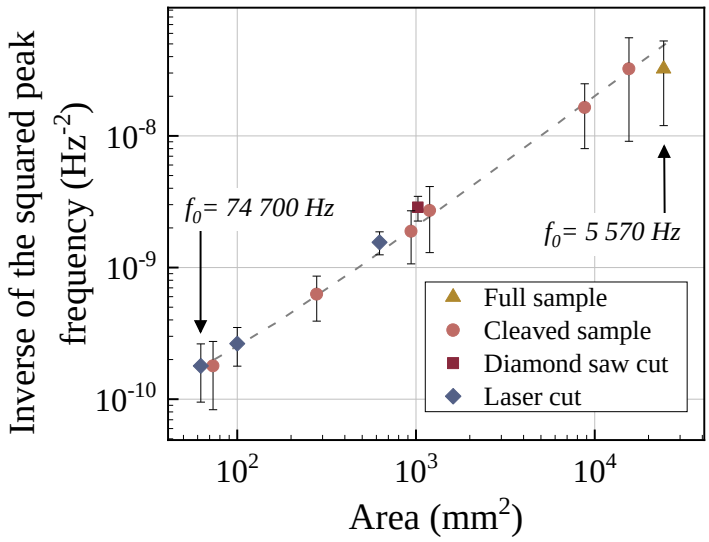

Figure 6: Inverse of squared f_o extracted from spectra presented in Fig. 5 as a function of the areas of the solar cells. The dashed line is a linear fit.

A solution to avoid this parasitic oscillation would thus be to reduce the cell area in order to push f_o out of the measurement bandwidth. However, this can increase the edge recombination current [14], hence modifying the behavior of the original device, especially if defects are introduced during the cutting. This being taken into account, reducing the size of the test samples can also present a real advantage for the analysis of the low frequency noise measured. Indeed, photovoltaic components being highly inhomogeneous (local contaminations, shunt resistances...), large test structures and complicate the noise analysis. As the theory of noise in solar cells is not very well developed yet, it is wise to limit the analysis to smaller components at first, in order to isolate and identify the noise source mechanisms in photovoltaic components, so as to characterize later on more standard size samples.

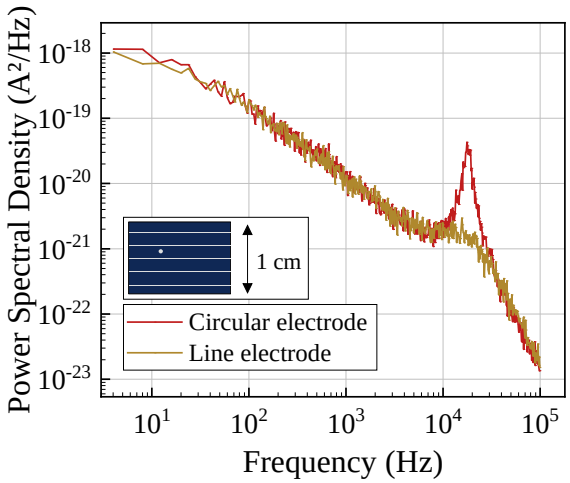

Figure 7 : Noise spectra measured on the same solar cell biased at V = 200 mV in forward with two types of electrodes, shown in the inset drawing.

Another solution is to modify the electrode patterns of the samples. Fig. 7 shows two noise spectra obtained from the same sample, with two different types of electrodes, a circular and a line-shaped one. It is clear that the circular electrode tends to limit the amplitude of the peak compared to the line-shaped electrode. This behavior was attributed to the higher R_s value introduced by the circular electrode, which is visible in the static curves shown in Fig 8. Indeed, the equivalent circuit's resonance quality factor is supposed to be reduced by the augmentation of R_S, thus reducing the amplitude of the peak. The trade-off in this case is the current degradation at high voltages which can compromise the proper performance characterization.

Despite these drawbacks, it is possible to fabricate solar cell structures, in terms of area and electrode shape, dedicated either for static or noise characterization and take into account the undesired side-effects during the LFN analysis.

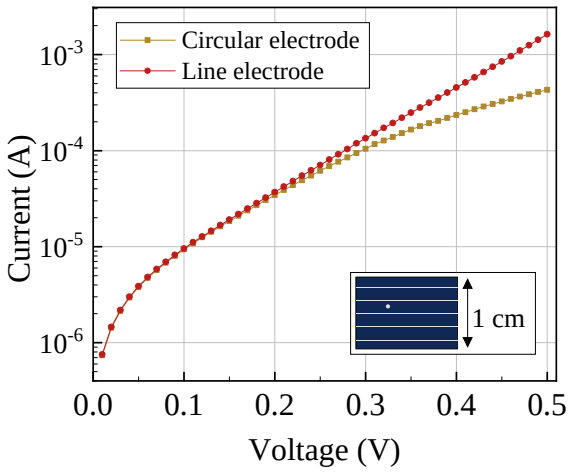

Figure 8 : Current-voltage curves obtained from measurements on the same solar cell with two type of electrodes, shown in the insert. Noise spectra at 200 mV are presented in Fig.7.

5. Conclusions

The parasitic oscillation observed in solar cell low-frequency noise characterization has been experimentally studied. The effect was attributed to the measurement circuit's instability in the presence of the large photodiode capacitance of the device under test. Certain solutions were proposed to overcome the presence of a peak polluting the noise spectrum measurement in some photovoltaic components, and limiting the analysis of low frequency noise. It was suggested to develop adapted test structures dedicated to noise measurement, either by reducing their surface and favoring some specific electrode patterns, in order to push further the oscillation frequency or reduce its amplitude, respectively. However, these solutions risk to modify the static behavior or performance of the devices and this must be accounted for in the noise characterization.

Acknowledgements

The authors would like to gratefully acknowledge the French National Research Agency for funding the Oxygen project (ANR-17-CE05-0035).

References

[1] R. Jayaraman, C.G. Sodini, 1/F Noise Technique To Extract the Oxide Trap Density Near the Conduction Band Edge of Silicon, IEEE Trans. Electron Devices. 36 (1989) 1773–1782. https://doi.org/10.1109/16.34242.

[2] R. MacKu, P. Koktavy, Analysis of fluctuation processes in forward-biased solar cells using noise spectroscopy, Phys. Status Solidi Appl. Mater. Sci. 207 (2010).

https://doi.org/10.1002/pssa.201026206.
[3] A. Bag, C. Mukherjee, S. Mallik, C.K. Maiti, Low frequency noise in polycrystalline p-β-FeSi2/Ge heterojunction solar cells, Proc. Int. Symp. Phys. Fail. Anal. Integr. Circuits, IPFA. 2 (2013) 377–380. https://doi.org/10.1109/IPFA.2013.6599185.
[4] C. Beguni, A.M. Cailean, S.A. Avatamanitei, M. DImian, Photodiode Amplifier with Transimpedance and Differential Stages for Automotive Visible Light Applications, in: 2020 15th Int. Conf. Dev. Appl. Syst. DAS 2020 - Proc., 2020. https://doi.org/10.1109/DAS49615.2020.9108928.
[5] S.T. Hsu, R.J. Whittier, C.A. Mead, Physical model for burst noise in semiconductor devices, Solid State Electron. 13 (1970). https://doi.org/10.1016/0038-1101(70)90102-4.
[6] M.J. Kirton, M.J. Uren, S. Collins, M. Schulz, A. Karmann, K. Scheffer, Individual defects at the Si:SiO2 interface, Semicond. Sci. Technol. 4 (1989) 1116–1126. https://doi.org/10.1088/0268-1242/4/12/013.
[7] T. Desrues, T. Michel, J.-F. Lerat, A. Veau, A. Lanterne, M. Coig, F. Milesi, F. Mazen, F. Torregrosa, L. Roux, S. Dubois, R. Monna, High quality industrial phosphorus emitter doping obtained with innovative plasma immersion ion implantation (PIII) processes, Proceeding 33rd Eur. Photovolt. Sol. Energy Conf. Exhib. Amsterdam. (2017).
[8] A. Hajimiri, T.H. Lee, A general theory of phase noise in electrical oscillators, IEEE J. Solid-State Circuits. 33 (1998) 179–194. https://doi.org/10.1109/4.658619.
[9] J. A. Chroboczek and G. Piantino, Programmable gain and bias low-noise current amplifier, France Patent No. 15075, 1999.
[10] J.G. Graeme, Photodiode Amplifiers: OP AMP Solutions, 1995.
[11] M. Boukadoum, A. Obaid, High-speed, low input current transimpedance amplifier for LED-photodiode pair, in: ICSPC 2007 Proc. - 2007 IEEE Int. Conf. Signal Process. Commun., 2007. https://doi.org/10.1109/ICSPC.2007.4728520.
[12] C.H. Chang, Z.M. Lin, A CMOS photo amplifier for living body real-time detection of free radical, in: 2013 IEEE Int. Conf. Electron Devices Solid-State Circuits, EDSSC 2013, 2013. https://doi.org/10.1109/EDSSC.2013.6628100.
[13] R. Costanzo, S.M. Bowers, A 10-GHz Bandwidth Transimpedance Amplifier with Input DC Photocurrent Compensation Loop, IEEE Microw. Wirel. Components Lett. 30 (2020). https://doi.org/10.1109/LMWC.2020.2993726.
[14] D. Bertrand, S. Manuel, M. Pirot, A. Kaminski-Cachopo, Y. Veschetti, Modeling of Edge Losses in Al-BSF Silicon Solar Cells, IEEE J. Photovoltaics. 7 (2017). https://doi.org/10.1109/JPHOTOV.2016.2618603.